



UNIVERSITY OF LEEDS

This is a repository copy of *Comparison of explosion characteristics of Colombian and Kellingley coal*.

White Rose Research Online URL for this paper:
<http://eprints.whiterose.ac.uk/105084/>

Version: Accepted Version

Proceedings Paper:

Huescar Medina, C, MacCoitir, B, Sattar, H et al. (3 more authors) (2014) Comparison of explosion characteristics of Colombian and Kellingley coal. In: 10th European Conference on Coal Research and its Applications. ECCRIA, 15-17 Sep 2014, Hull, UK. .

Reuse

Unless indicated otherwise, fulltext items are protected by copyright with all rights reserved. The copyright exception in section 29 of the Copyright, Designs and Patents Act 1988 allows the making of a single copy solely for the purpose of non-commercial research or private study within the limits of fair dealing. The publisher or other rights-holder may allow further reproduction and re-use of this version - refer to the White Rose Research Online record for this item. Where records identify the publisher as the copyright holder, users can verify any specific terms of use on the publisher's website.

Takedown

If you consider content in White Rose Research Online to be in breach of UK law, please notify us by emailing eprints@whiterose.ac.uk including the URL of the record and the reason for the withdrawal request.



eprints@whiterose.ac.uk
<https://eprints.whiterose.ac.uk/>

1 **Proceedings of the 10th European Conference on Coal Research and its Applications**
2 **10th ECCRIA**

3
4 Huescar-Medina, C., Andrews, G.E., Phylaktou, H.N. and Gibbs, B.M., Comparison of
5 explosion characteristics of Columbian coal and Kellingley Coal. Proceedings of the 10th
6 European Conference on Coal Research and its Applications, University of Hull, 2014.
7

8
9 **TITLE:** Comparison of explosion characteristics of Colombian coal and Kellingley coal

10 **AUTHORS:** Huescar Medina (2 surnames), Clara*; MacCoitir, Brian; Sattar, Hamed; Slatter, D.,
11 Phylaktou, Herodotos N.; Andrews, Gordon E.; Gibbs, Bernard M.

12 **AFFILIATION:** Energy Research Institute, School of Chemical and Process Engineering, University
13 of Leeds, Leeds, LS9 2JT, United Kingdom

14 ***CORRESPONDING AUTHOR:**

15 Tel. (+44) 07879372345

16 Email: pm09chm@leeds.ac.uk

17 Address: Energy Research Institute, University of Leeds, Leeds, LS9 2JT, United Kingdom

18 **Abstract**

19 Coal continues to be one of the main fuels used for generation of energy in the UK. Despite
20 government's plans to decarbonise the energy sector to comply with emission targets, co-firing of coal
21 and biomass, due to the low investments required, is one of the most attractive methods to do so.
22 Additionally, if gas prices remain high, the resulting consumption of coal is still considerable.
23 Pulverised coal has been known to pose explosion risks since the 19th century. The objective of the
24 present work was to compare the explosibility of two samples of bituminous coal used in UK power
25 stations which potentially can be used co-fired with biomass. The 1 m³ ISO explosion vessel was used

26 to determine the explosion characteristics: deflagration index (K_{St}), maximum explosion pressure
27 (P_{max}) and minimum explosible concentration (MEC). Other fundamental combustion properties such
28 as flame speeds, global heat release rates and burning velocities were measured. Remaining residues
29 collected after explosion tests were also analysed. Despite the similarities in composition of both
30 coals, the explosion reactivity of Colombian coal was much higher, with a K_{St} value of 129 barsm^{-1} as
31 opposed to 73 barsm^{-1} for Kellingley coal. Main differences between fuels were the surface area of
32 particles and char burnout rates which were higher for Colombian coal. This suggests that the physical
33 properties of coal particles can significantly contribute to the explosibility of coal fuels.

34 **KEYWORDS:** coal, dust explosion, combustion, flame propagation, biomass

35 1. Introduction

36 Coal is the major fuel used for generating electricity worldwide. In 2012 coal was used to generate
37 41% of the world's electricity [1]. In the UK, despite the introduction of renewable fuels for GHG
38 emission reduction, 29% of the electricity generated is still produced from coal [2]. Pulverised coal
39 combustion is the most commonly used method in coal-fired power plants [3]. It was back in the 19th
40 century that coal dust clouds were first ignited by electric sparks. Since then extensive research efforts
41 have been devoted to understand coal dust explosibility and flame propagation [4]. Coal power plants
42 present explosion risks in milling processes, transport of fuel to the boiler and during operation, start
43 up and shut down of the boiler [5]. As a result these plants must comply with ATEX and DSEAR
44 regulations to prevent or limit the effects of explosions. The design of safety systems such as venting
45 or suppression systems requires the knowledge of the explosion characteristics of any hazardous dust.
46 Explosion characteristics include: the deflagration index (K_{St}), the maximum explosion pressure
47 (P_{max}), minimum explosion concentration (MEC) amongst others (limiting oxygen concentration,
48 minimum ignition energy, etc.). The methods for determination of all explosion characteristics are
49 outlined in the standard EN BS 14034. For the determination of K_{St} , P_{max} and MEC, which are
50 considered in this study, explosion tests are performed in a 1 m^3 explosion vessel within the

51 flammable range. Pressure-time histories are recorded. Deflagration index (K_{St}) is derived according
 52 to the cube-root law:

$$K_{St} = \left(\frac{dP}{dt} \right)_{max} \cdot V^{1/3} \quad (1)$$

53

54 K_{St} and P_{max} are determined as a function of concentration and maximum values measured are used in
 55 design calculations for protection systems.

56 The explosion characteristics of many types of coal have been determined. In the early days a lot of
 57 data was gathered for carbonaceous dusts using vertical tube apparatuses such as the Hartmann tube
 58 [5, 6]. More recent studies [7-12] used current standard methods for the characterisation of coal
 59 explosibility. Results obtained in such studies are shown in Table 1.

60 **Table 1. Explosion characteristics of different coal samples in the literature**

Coal sample	K_{St}	P_{max}	MEC	Vessel volume	Ref.
Morwell coal	220	7.6	-	20 L	[11]
Brown coal	151	10.0	-	1 m ³	
Yallourn dark	91	6.7	-	20 L	
Prince mine coal	44	6.5	70	20 L	[12]
Phalen mine coal	30	6.0	120	20 L	
Lingan mine coal	44	7.0	90	20 L	
Russian anthracite	68	5.0	-	20 L	[10]
Sulcis lignite	162	6.8	-	20 L	
South African coal	81	6.0	-	20 L	
Polish coal	135	6.8	-	20 L	
Snibston coal	149	6.5	-	20 L	
Spanish lignite	107	8.8	90	1 m ³	[13]
German lignite	105	8.7	60	1 m ³	
Pittsburgh coal	41	6.7	65	20 L	[8]
Pocahontas coal	31	6.5	80	20 L	
Sebuku coal	114	6.6	63	20 L	[14]

61 According to literature values for a diverse range of coal samples containing fine particles (<75 µm),
 62 the explosion characteristics of coals can vary widely. K_{St} values range from 30 barsm⁻¹ to 220 barsm⁻¹

63 ¹, P_{\max} from 5 bar to 10 bar and MECs from 60 gm^{-3} to 120 gm^{-3} . This variability is due to the diverse
64 composition of different coals.

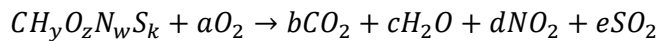
65 Coal dust flame propagation mechanisms have also been the object of research. It is generally
66 accepted that the combustion process of coal particles consists of devolatilisation and subsequent
67 reaction of volatile components, heterogeneous surface reactions as well as other physiochemical
68 changes to the particles [15]. These processes are not only affected by the coal type, dust
69 concentration and particle size distribution but by the heating rate, final temperature, residence time
70 and quench process [16]. The heating rate of explosion events is considered to be high as is the
71 maximum temperature [17]. Therefore coal particles burning in dust clouds undergo fast pyrolysis.
72 Hertzberg et al. [18] suggested that the char oxidation rate is too slow to make a significant
73 contribution to flame propagation and therefore considered that char acted as a heat sink. This
74 approach has been considered for the modelling of coal dust explosions more recently [17, 19].
75 However, other researchers pointed out that this model fails to consider the possible effects of particle
76 structure on explosibility [9, 11]. Woskoboenko [11] suggested that the surface area of certain coals
77 could greatly affect the explosion reactivity as the rates of devolatilisation and char burnout are faster.
78 The objectives of the present work were to measure the explosion characteristics (MEC , K_{St} , P_{\max}) of
79 pulverised Colombian coal and Kellingley coal and study the effect of surface area on such
80 characteristics and determine combustion properties like laminar and turbulent flame speeds, burning
81 velocity and global heat release rate (which can in turn be used in the design of combustion systems).
82 In addition residues collected after explosion tests were analysed in order to understand its origin and
83 its role in the explosion event.

84 **2. Experimental methods**

85 **2.1. Fuels and their characterisation**

86 Samples of Colombian and Kellingley coal were supplied in pulverised form by Moneypoint (Ireland)
87 and Drax (UK) power stations respectively. The original fuels and some samples of residue collected

88 after explosion tests were analysed for their composition through elemental and TGA-proximate
 89 analysis using a Flash 2000 Thermoscientific C/H/N/S analyser (oxygen content was calculated by
 90 subtraction), and a TGA-50 Shimadzu analyser respectively. The elemental composition was used to
 91 derive the stoichiometric fuel to air ratio. Assuming the fuel formula is $CH_yO_zN_wS_k$ where y, z, w and
 92 k are the atomic ratios to carbon of hydrogen, oxygen, nitrogen and sulphur respectively, and
 93 assuming the combustion reaction was:



94 The stoichiometric fuel to air mass ratio was given by:

$$\text{Stoichiometric } (F/A) = \frac{(12 + y + 16z + 14w + 32k)}{\left[\left(1 + \frac{y}{4}\right) - \frac{z}{2} + w + k\right] \cdot \frac{32}{0.232}} \quad (2)$$

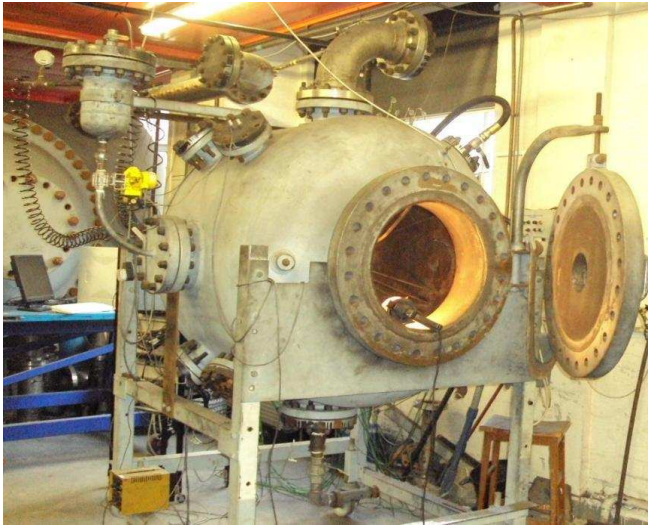
95 The stoichiometric (F/A) ratio can be expressed as grams of fuel per cubic meter of air by multiplying
 96 the stoichiometric fuel to air mass ratio by the density of air (1200 gm^{-3}). In addition, the
 97 concentration of dust clouds was expressed as an equivalence ratio (ratio of actual to stoichiometric
 98 concentrations). The gross calorific value (GCV) of all samples was determined in a Parr 6200 bomb
 99 calorimeter to the specifications of BS ISO 1928:2009 [20]. Bulk densities of all pulverised fuels were
 100 determined weighing increasing amounts of fuels in a known volume. The results were expressed as
 101 the average of 10 measurements. Furthermore, the density of particles (true density) was measured
 102 using an AccuPyc 1330 Pycnometer.

103 The morphology of particles before and after explosion was assessed through Scanning Electron
 104 Microscopy (SEM) images using a Carl Zeiss EVO MA15 instrument and the particle size
 105 distributions were determined using a Malvern Mastersizer 2000 instrument.

106 The surface area and porosity of fuels were also determined through Brunauer–Emmett–Teller (BET)
 107 analysis in a Micrometrics Tristar 3000 analyser. The analysis gas used was Nitrogen, and all samples
 108 were prepared (degassed) at $120 \text{ }^\circ\text{C}$ for 4 hours.

109 **2.3. Explosion characterisation: ISO 1 m³ vessel**

110 Explosion tests were performed using the ISO 1 m³ vessel according to the methods recommended by
111 the European standard EN BS 14034. The set-up consisted of a 1 m³ volume explosion chamber
112 connected through a 19 mm internal diameter pipe to an external 5 L dust holder (Fig.1).



113

114 **Figure 1: Leeds ISO 1 m³ vessel**

115 Initially the dust sample was loaded into the external dust holder and pressurized to 20 bar. A fast
116 acting valve separated both the dust holder and explosion chamber. On activation of the valve the dust
117 was pushed through the delivery system and dispersed inside the explosion chamber through the
118 standard C-tube. After an ignition delay of 0.6 s from the start of dust dispersion into the vessel,
119 ignition of the dust took place by means of two 5 kJ chemical igniters placed in the geometric centre
120 of the explosion chamber, firing into a perforated hemispherical cup to ensure central ignition and
121 spherical propagation, as far as possible. Prior to dispersion of the dust from the dust holder, the
122 explosion chamber was evacuated so that on addition of the dust from the dust holder, the initial
123 pressure at the time of ignition was 1.013 bar.

124 After an explosion in the 1 m³ vessel, dust residues were found both in the dust holder (not dispersed)
125 and in the explosion chamber. The dust found in the dust holder did not participate in the combustion
126 reaction and therefore it was accounted for to correct the amount of dust present inside the explosion

127 chamber (injected concentration). However, the dust that remained in the explosion chamber was a
128 mixture of burnt, partially burnt and unburnt material. All residues were collected and quantified but
129 only the residue found for the most reactive concentration was analysed.

130 The vessel was fitted with Keller PA11 piezoresistive pressure transducers for recording of pressure-
131 time histories and also with arrays of exposed junction type-K thermocouples in the horizontal (left
132 and right) and vertical (downwards) directions. These thermocouples allowed determination of times
133 of flame arrival to each thermocouple position and derivation of flame speeds in all directions. The
134 overall radial turbulent flame speed $(S_F)_T$ for a given test was the average of the flame speed in each
135 direction. K_{St} was computed from the maximum rate of pressure rise obtained by combustion in the 1
136 m^3 volume closed vessel according to Eq.(1). The maximum pressure and the maximum rate of
137 pressure rise for a given mixture were derived from the pressure-time histories. The maximum
138 pressure for a given mixture of dust was normalised for the initial pressure at the time of ignition (P_1).

139 Turbulent flame speeds were derived from the tests. Turbulent $(S_F)_T$ and laminar (S_F) flame speeds are
140 related as follows [21],

$$(S_F)_T = \beta \cdot S_F \quad (3)$$

141 where β is the turbulence factor of the vessel. β is a parameter used in venting correlations to account
142 for the turbulence created by obstacles in the path of the flame. Here it was used to account for the
143 turbulence induced due to the dispersion of dust. β was found to be 4.03 for the Leeds 1 m^3 ISO vessel
144 by performing laminar and turbulent gas explosions by adding pressurized air from the dust pot,
145 which provided an analogous turbulence to that present in dust explosions. Additionally, approximate
146 laminar burning velocities could be derived from the flame speed measurements. The relationship of
147 flame speed and burning velocity us given by:

$$S_F = S_L \cdot E$$

148 Where E is the expansion factor, ratio of densities of unburnt and burnt gases. Flame speeds are
149 measured between 200 and 800 mm diameter in the vessel at constant pressure and the expansion
150 factor at constant pressure can be approximated by the pressure ratio. For dusts, obtaining the
151 expansion factor at constant pressures is often problematic and therefore it is usually replaced by the
152 measured pressure ratio P_{max}/P_i . Laminar burning velocities were therefore derived from turbulent
153 flame speed measurements using the following expression:

$$S_L = \frac{(S_F)_T}{\beta \cdot (P_{max}/P_i)}$$

154 The MW per unit area of the flame front (heat release rate or HRR) was calculated using the
155 following expression:

$$HRR \left(MW/m^2 \right) = \frac{(S_F)_T}{\left(\frac{P_{max}}{P_i} \right)} \rho_u \frac{GCV}{(1 + A/F)}$$

156 Where ρ_u was taken as the unburnt air density 1.2 kgm^{-3} and A/F was the corresponding air to fuel
157 ratio.

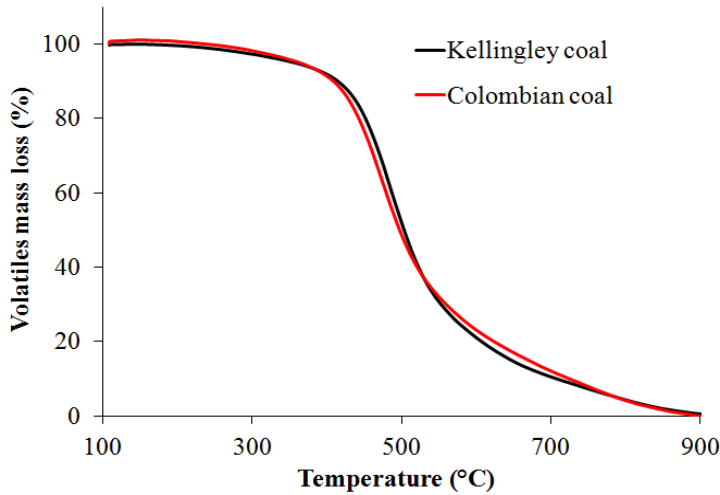
158 **3. Results and discussion**

159 **3.1. Fuel characterisation**

160 Characteristics of both fuels are shown in Table 2. Main difference between both bituminous coal
161 samples was found on the particles surface area. The surface area of Colombian coal particles was
162 found to be 4.3 times higher than that of Kellingley coal. The pore volume for Colombian coal was
163 also more than two times higher than that of Kellingley coal. In regards to the elemental and
164 proximate analysis, Colombian coal contained 67% less sulphur than Kellingley coal and more
165 oxygen (36%), volatile matter (15%) and moisture (88%). Overall the stoichiometry of the coal
166 samples was virtually the same.

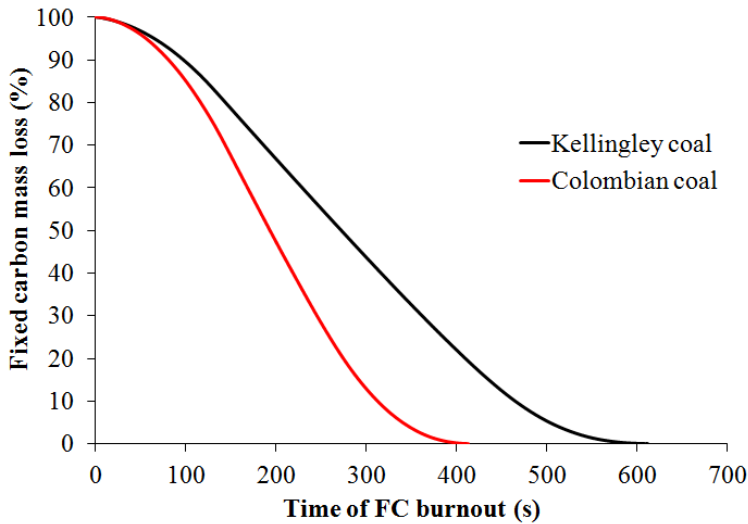
	Kellingley coal	Colombian coal
Bulk density (kgm^{-3})	443	407
True density (kgm^{-3})	1480	1450
Surface area (m^2g^{-1})	3.7	15.8
Pore volume cm^3g^{-1}	0.014	0.032
GCV (MJkg^{-1}) _{daf}	33.8	33.5
Elemental Composition (w/w, daf)		
C	82.1	81.8
H	5.2	5.3
N	3.0	2.5
S	2.8	0.9
O	7.0	9.5
Proximate analysis (w/w, as received)		
Moisture	1.7	3.2
VM	29.2	33.7
FC	50	47.8
Ash	19.1	15.3
Stoichiometric (A/F)	11.3	11.1
Stoichiometric F/A (gm^{-3})	106	108

168 Mass loss and rate of mass loss curves during Proximate-TGA analysis were compared. Weight loss
169 curves were separated and normalised for volatile release related mass loss (Fig.2) and fixed carbon
170 mass loss (Fig.3). These steps occurred in inert and oxidative atmospheres respectively.



171

172 **Figure 2. Volatiles mass loss of Kellingley and Colombian coal**

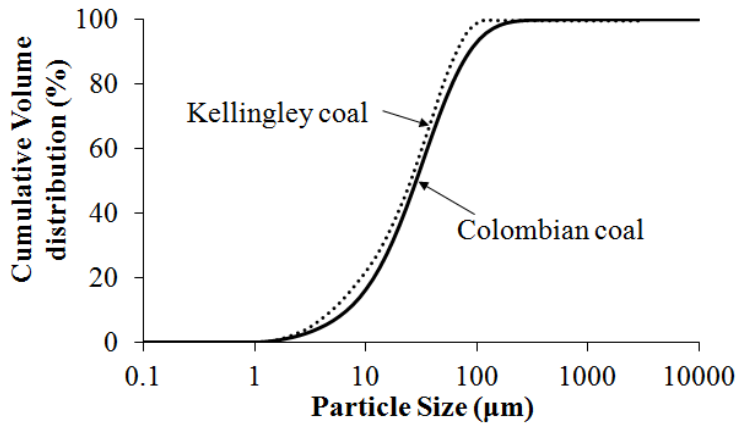


173

174 **Figure 3. Fixed carbon mass loss of Kellingley and Colombian coal**

175 Both coals presented very similar rate of mass loss due to volatiles release, however, on oxidation of
 176 the remaining char after volatile release, the rate of mass loss was almost two times faster for
 177 Colombian coal. The higher surface area of Colombian coal clearly enhanced the rate at which the
 178 char was burnt and is likely that in an oxidative environment the rate of devolatilisation and volatile
 179 combustion would be faster as well.

180 The particle size of both coals was also studied and the results showed that fuels contained particles of
 181 very similar size. Fig.4 shows the cumulative volume distribution for both samples. Table 3 shows the
 182 comparison of size parameters of the samples.



183

184 **Figure 4. Cumulative volume distribution of Kellingley and Colombian coal**

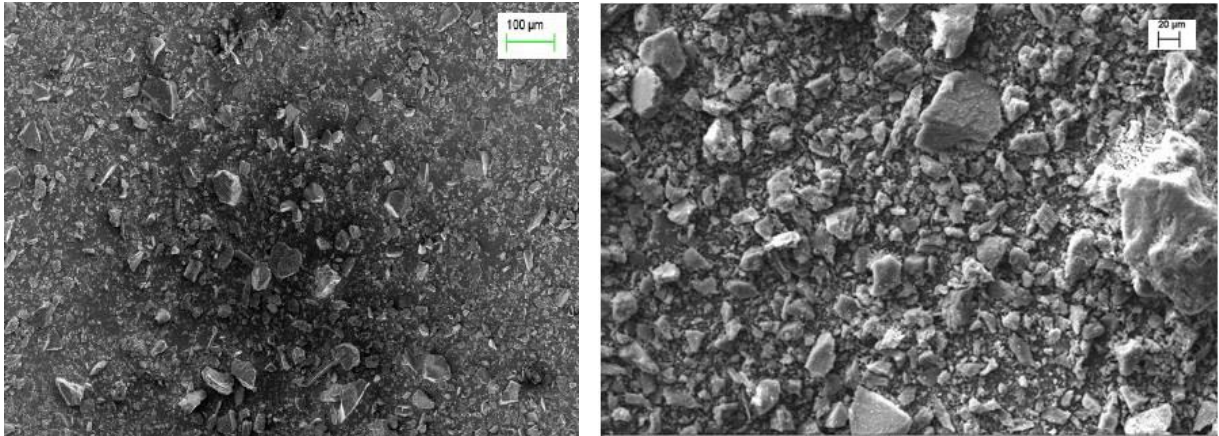
185 **Table 3. Particle size analysis parameters**

	Surface weighted mean diameter $D[3,2]$ (μm)	Volume weighted mean diameter $D[4,3]$ (μm)	D_{10} (μm)	D_{50} (μm)	D_{90} (μm)
Kellingley Coal	12	31	5.0	25.5	65.3
Colombian coal	15	40	6.8	28.1	85.2

186 SEM images were used to assess the morphology of coal particles of both samples. Coal particles
 187 typically present angular and sharp edges [22, 23]. Fig.5 present SEM images of Kellingley and
 188 Colombian coal were the characteristic features of coal particles are confirmed.

Kellingley coal (x300)

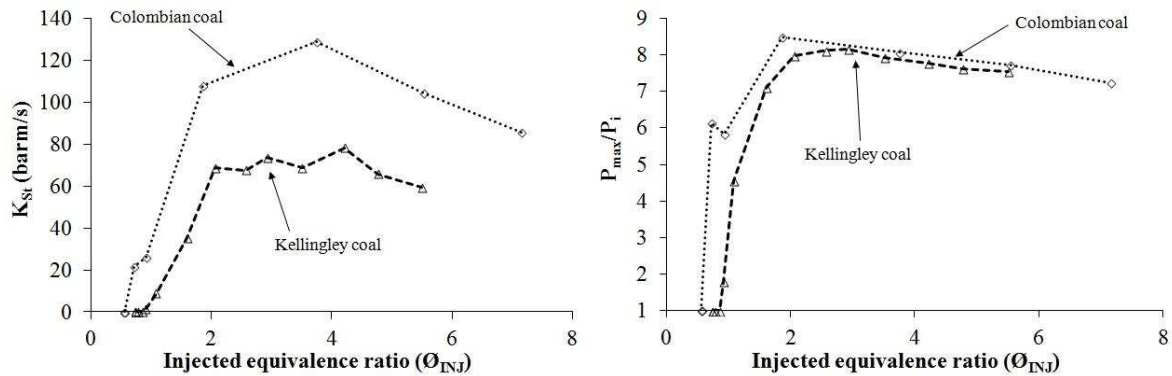
Colombian coal (x500)



189 **Figure 5. SEM images of Kellingley (left) and Colombian (right) coal**

190 **3.2. Explosion characterisation**

191 K_{St} and pressure ratios are presented in Fig.6 as a function of the injected equivalence ratio.
 192 Colombian coal presented a maximum K_{St} value which was 1.7 times higher than that of Kellingley
 193 coal. This also indicated faster rate of combustion. Maximum explosion pressure for Colombian coal
 194 was 8.5 bar and 8.2 bar for Kellingley coal. In comparison to K_{St} literature values for other coal types,
 195 Colombian coal was similar to the more reactive coals reported and Kellingley coal to the least.



196

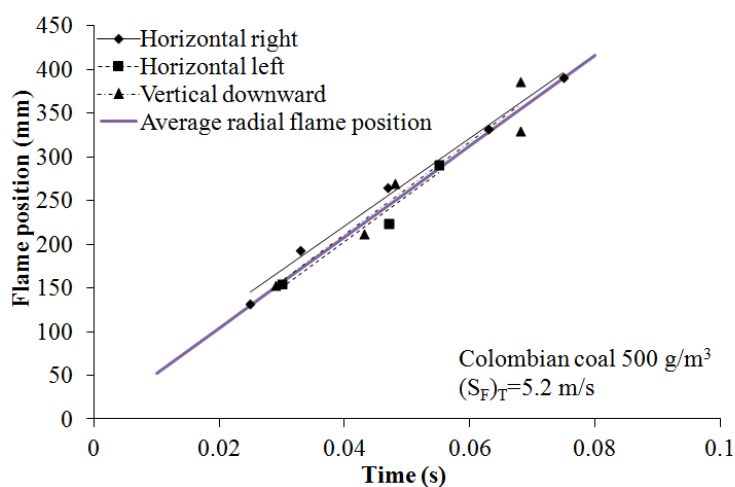
197 **Figure 6. K_{St} and pressure ratio as a function of injected equivalence ratio**

198 Despite the similarities in composition, the reactivity in terms of K_{St} of Colombian coal was found to
 199 be significantly higher than that of Kellingley coal. The maximum pressure is dependent on the
 200 energy content of the fuel/air mix and the heat losses. Since both samples had similar calorific values
 201 the difference in maximum pressure was not large. The greater difference in K_{St} indicates that the rate

202 of mass burning was markedly different for each of the samples. The rate of mass burning in this case
 203 is most likely affected by surface area. It was pointed out in section 3.1 that the surface area of
 204 Colombian coal was distinctly higher than that of Kellingley coal. It is generally accepted that when
 205 heating rates are high the amount of volatiles release is increased in comparison to that detected under
 206 proximate analysis techniques. The increase of volatiles due to high heating rates should be similar for
 207 both samples. However, the rate of volatile release and combustion could be enhanced due to the
 208 higher surface area of Colombian coal. The rate of char burnout could also have been increased due to
 209 the surface area which overall resulted in an increase of the rate of combustion and therefore the rate
 210 of pressure rise and K_{St} .

211 The minimum explosive concentration (injected) for Kellingley coal was 91 gm^{-3} and 60 gm^{-3} for
 212 Colombian coal. These values confirmed the reactivity trend and were similar to MEC values found in
 213 the literature for coals. The correspondent equivalence ratios for Kellingley and Colombian coal were
 214 $\phi=0.82$ and $\phi=0.56$ respectively, using the solid fuel stoichiometry.

215 Flame speeds were measured using the thermocouple arrays fitted to the 1 m^3 explosion vessel. An
 216 example of a flame position plot obtained for Colombian coal is shown in Fig.7. The position of the
 217 flame over time was mapped out in three directions: horizontal right and left and vertical downwards.



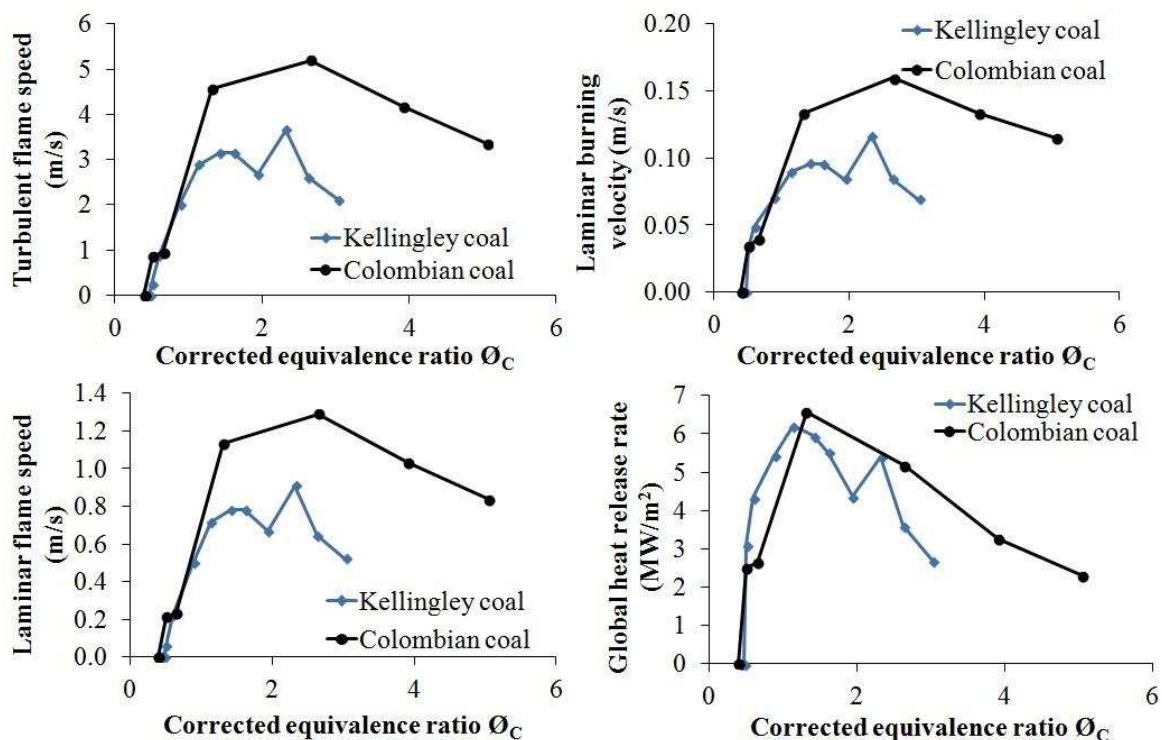
218

219 **Figure 7. Example flame position graph and derivation of flame speeds**

220 The slope of a linear fit to the positions in each direction corresponded to the flame speed in such
 221 direction. The average flame speed for a single test is the average of the flame speeds in each
 222 direction and is represented in Fig.7 by the average radial flame position line.

223 The maximum flame speed for Kellingley coal was 3.7 m/s, whereas it was 5.2 m/s for Colombian
 224 coal. Using the turbulence factor obtained for this explosion vessel (4.03) the corresponding laminar
 225 flame speeds were 0.9 m/s and 1.3 m/s. These values are comparable to values quoted in the literature
 226 for other coals [15].

227 Figure 8 shows the variation of flame speeds (turbulent and laminar), burning velocity and heat
 228 release rate for a range of mixtures within the flammable range. Typical pf boilers produce heat
 229 release rates of around 3-6 MWm⁻² at typical conditions of 20% excess air [24, 25]. At such
 230 conditions, the heat release rate obtained for Kellingley coal was around 3 MWm⁻² and 5 MWm⁻² for
 231 Colombian coal. These values are comparable to typical heat release rates obtained in pulverised fuel
 232 boilers and therefore combustion data produced in the 1 m³ explosion vessel is applicable to burner
 233 design.



235 **Figure 8. Turbulent and laminar flame speeds, laminar burning velocities and heat release rate**
236 **of Kellingley and Colombian coal**

237 **3.3. Analysis of residues**

238 Residues collected after explosion tests of the most reactive concentrations were further analysed
239 following the same procedures as for the original samples. In explosion tests with coal it was not
240 possible to distinguish visually whether particles were burnt or unburnt. However, in previous work
241 carried out with woody biomass samples by the Leeds group [26] it was found that residues formed a
242 layer where the particles closest to the wall appeared unreacted and particles exposed presented signs
243 of being burnt.

244 Assuming that the layer of residue was homogeneously distributed in the vessel walls and considering
245 the vessel spherical and since the density and mass of residue were known a theoretical layer
246 thickness was calculated. The thickness of the layer increased as more dust was present in the vessel
247 (see Fig.9).

248 Additionally, the rate of pressure loss could also be calculated using the pressure-time histories. The
249 rate of pressure loss was defined as:

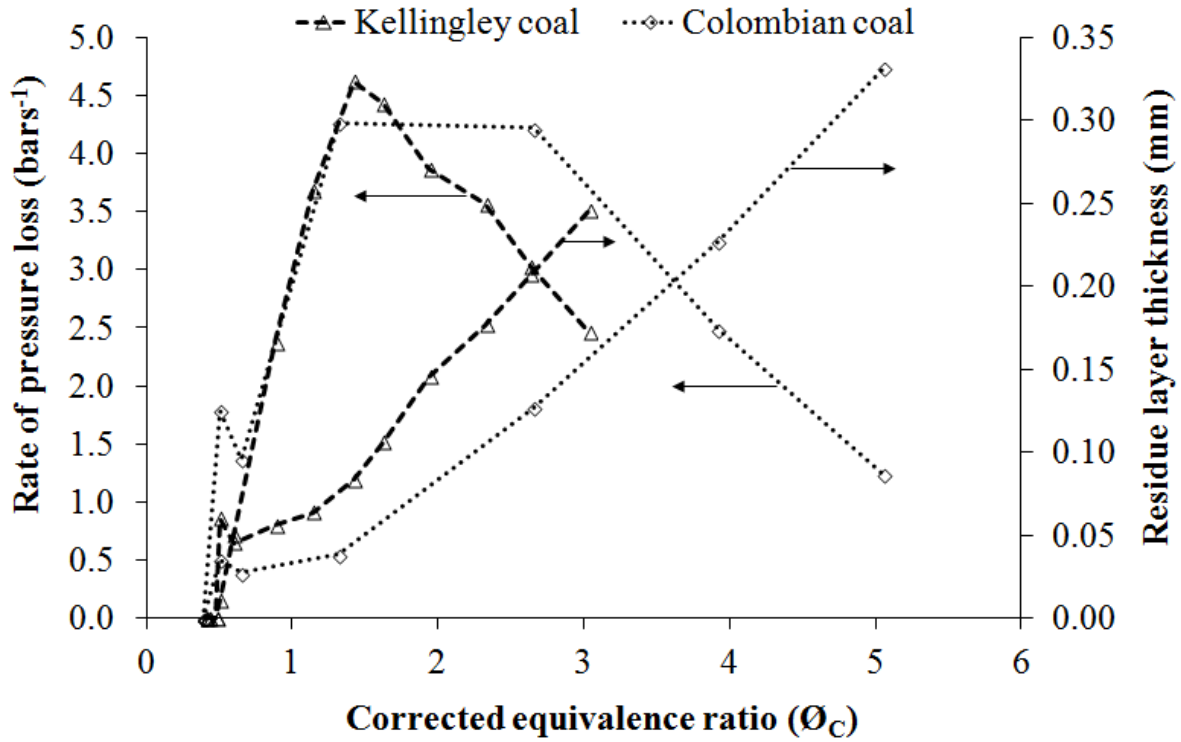
$$\text{Rate of pressure loss} = \frac{P_{max} - 0.9P_{max}}{\Delta t} \quad (4)$$

250 Rates of pressure loss and layer thicknesses for Kellingley and Colombian coal are shown in
251 Fig.9. The rate of pressure loss increases initially as flame temperature increased. However, after the
252 maximum flame temperatures are achieved for mixtures slightly richer than stoichiometric the
253 pressure loss decreased. It is known from the maximum explosion pressure plot (Fig. 6, right) that
254 pressure remains fairly constant for mixtures around 2 times rich which indicates that flame
255 temperatures also remained fairly constant. Therefore, for rich mixtures the decrease in rate of
256 pressure loss should have remained constant. However, because the thickness of the layer created was

257 increasingly thicker as more dust was injected the rate of pressure loss decreased.

258

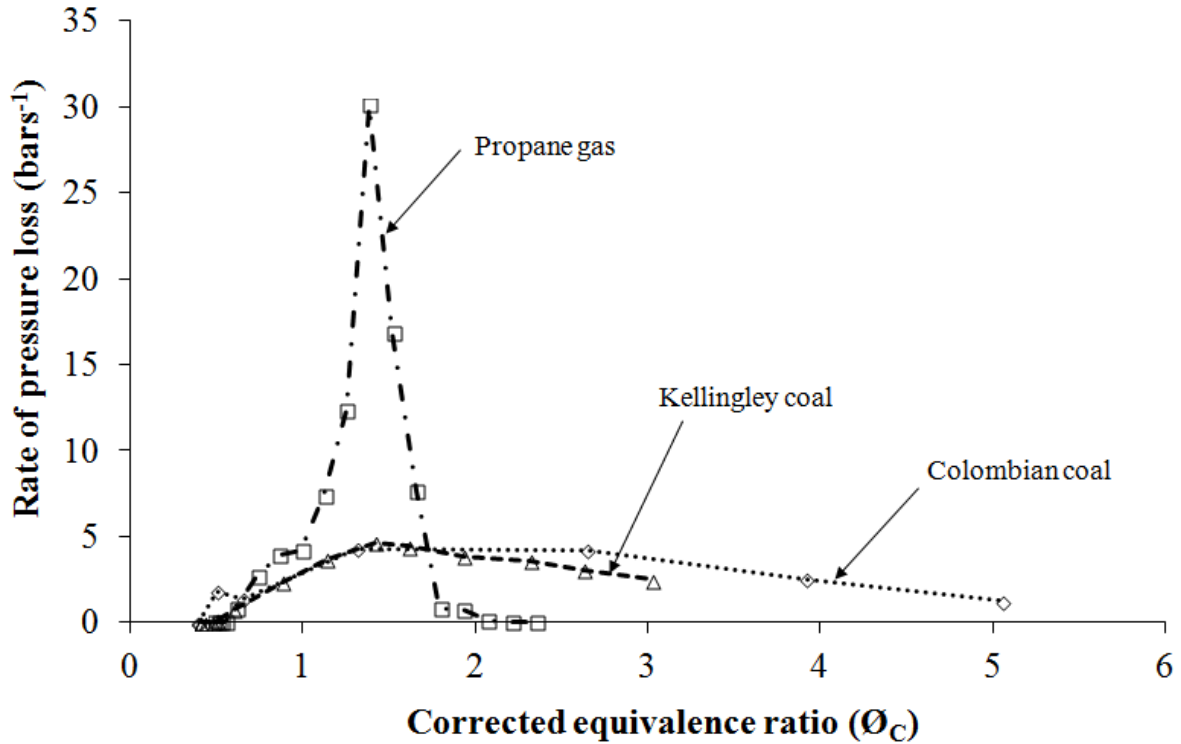
259



260

261 **Figure 9. Rates of pressure loss and layer thickness as a function of corrected (burnt)**
262 **equivalence ratio**

263 This phenomenon was found to be different when gas explosions were performed in the same 1m³
264 explosion vessel. Figure 10 shows a comparison of the rate of pressure loss between gas propane and
265 the two coal dusts used in this study. The maximum rate of pressure loss with gases was much higher
266 since no insulating layer was formed and heat was lost faster through the vessel walls. Furthermore,
267 the rate of pressure loss decayed for rich mixtures as maximum flame temperatures decreased.



268

269 **Figure 10. Comparison of rates of pressure loss of gas propane and coal dusts**

270 Previous work by the Leeds group used a density separation method to isolate burnt, partially burnt
 271 and unreacted particles. However, in this study the residue samples were analysed as a bulk. Table 4
 272 presents the elemental and proximate analysis of original samples and residue samples. The
 273 percentage of change respect the original sample is presented between brackets. The elemental
 274 composition of the residues was different from that of the original sample. According to the proximate
 275 analysis volatiles were lost. The variations in elemental composition were therefore due to the loss of
 276 volatiles. Interestingly, the overall content of oxygen increased for Kellingley coal whereas it
 277 decreased by 65% for Colombian coal. This indicates that oxygen in Colombian coal was present in
 278 bonds which were easily broken. This coupled with the higher surface area leading to faster rates of
 279 reaction resulted in Colombian coal having higher reactivity.

280 Another consistent feature of the residues was that both ash and fixed carbon contents increased for
 281 both fuels. All these trends point to residues undergoing pyrolysis inside the vessel and support the
 282 theories suggested in [26] where by residues were a proportion of the injected dust which was pushed

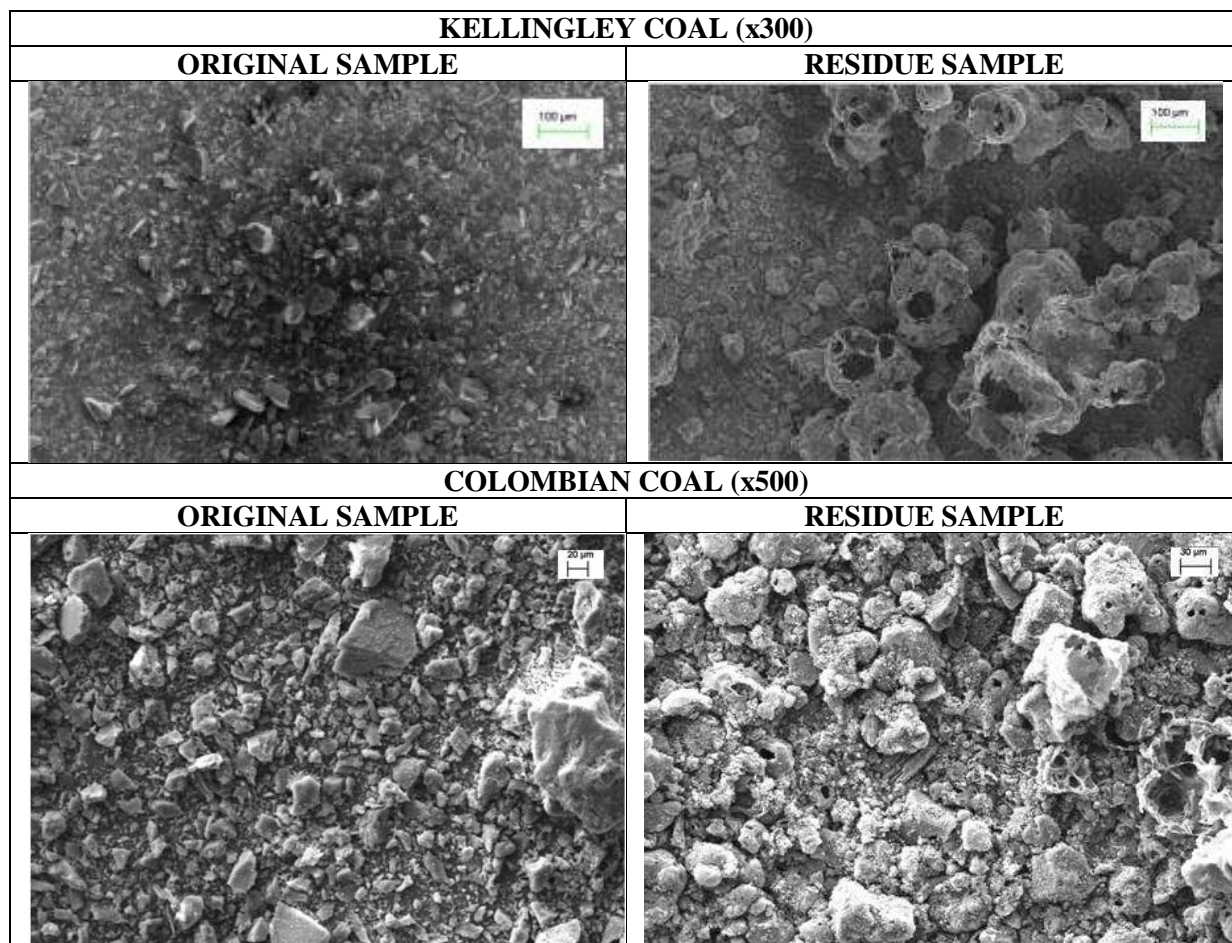
283 by the explosion wind towards the vessel wall (this was proven by measuring the rates of pressure loss
 284 in gas and dust tests). It has been shown that the rate of pressure loss in gas tests was much faster than
 285 with dusts, where a layer of dust acted as insulator. At the wall, the flame front impinges in the outer
 286 layer of dust momentarily as the flame is quenched by conduction through the walls. However, the top
 287 layer closest to the impinging flame front was partially pyrolysed. This detail is reflected in the bulk
 288 residue analysis carried out here.

289 **Table 4. Analysis of most reactive mixture explosion residue of Kellingley coal and Colombian**
 290 **coal**

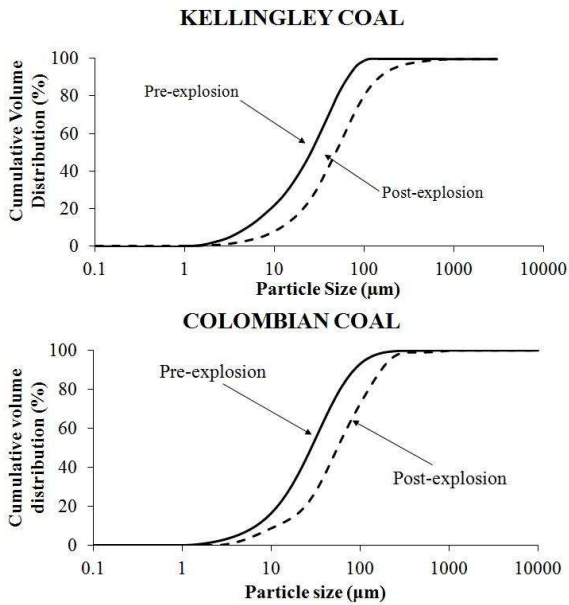
	Pre-Explosion	Post-Explosion
Fuel Sample	Kellingley coal	Kellingley coal (Change %)
Elemental analysis (% by mass) _{daf}		
C	65.0	64.3 (-1)
H	4.1	3.5 (-15)
O	5.5	7.1 (+29)
N	2.4	1.4 (-42)
S	2.2	2.2
TGA-Proximate (% by mass)		
Moisture	1.7	1.6 (-6)
Ash	19.1	19.9 (+4)
Volatile Matter	29.2	25.0 (-14)
Fixed Carbon	50.0	53.5 (+7)
Fuel Sample	Colombian coal	Colombian coal (Change %)
Elemental analysis (% by mass) _{daf}		
C	66.6	61.8 (-7)
H	4.3	2.1 (-51)
O	7.8	2.7 (-65)
N	2.1	1.7 (-19)
S	0.7	0.9 (+29)
TGA-Proximate (% by mass)		
Moisture	3.2	2.2 (-31)
Ash	15.3	28.5 (+86)
Volatile Matter	33.7	14.4 (-57)
Fixed Carbon	47.8	54.9 (+15)

291 Further prove to the theory is given by the SEM images of the samples after explosion tests (see
 292 Figure 10). SEM images of the residues (right images) show that original particles are mixed with
 293 bigger and structurally different char particles. This confirms that a layer of particles likely to be
 294 closest to the wall when the flame front impinged remained unchanged. Char particles (closest to the

295 flame front) became molten and formed large clusters of round surfaces with blow out holes as had
296 been previously reported in the literature [22, 23]. As a result to the formation of char, the overall size
297 distribution of residues presented larger particles than the original sample. This is shown in Fig.11.



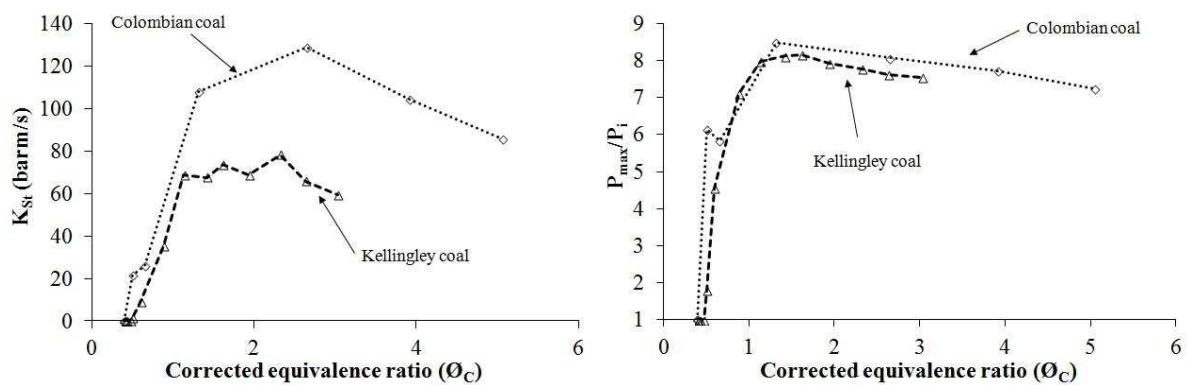
298 **Figure 11. SEM images of original and residual samples of Kellingley coal and Colombian coal**



299

300 **Figure 12. Particle size distribution of original and residual samples of Kellingley coal and**
 301 **Colombian coal**

302 As residue analysis seemed to indicate the dust pushed against the wall did not participate in the
 303 explosion reaction. As the weight of residues is logged as part of the test procedures, corrections can
 304 be applied to injected concentrations to define the most accurate burnt concentration and equivalent
 305 ratio. This is reflected in Fig.12 for the reactivity plots of K_{St} and maximum pressures.



306

307 **Figure 13. K_{St} and maximum pressure as a function of corrected (burnt) equivalence ratio**

308 The MEC could also be corrected, in which case the corresponding MEC concentration for
 309 Colombian coal was 43 gm^{-3} ($\text{Ø}=0.4$) and for Kellingley coal 50 gm^{-3} ($\text{Ø}=0.5$).

310 **Conclusions**

311 The explosion reactivity, in terms of K_{St} , P_{max} and MEC, of two samples of coal currently used in
312 power stations (Kellingley coal and Colombian coal) was studied. Explosion characteristics of both
313 samples fell within the somewhat wide range of values available in the literature. Despite having very
314 similar composition samples presented different explosion reactivity. The rate of reaction was
315 enhanced for the sample of Colombian coal due to the high surface area of the particles. Maximum
316 pressures, MECs and flame speeds measured also reflected the difference in reactivity. This proves
317 that particle structure can influence the rate of the combustion reaction and therefore the explosion
318 reactivity of coal. The results also suggest that the heterogeneous combustion step might contribute to
319 the overall combustion reaction more than originally considered.

320 The analysis of bulk residues reflected that some of the particles were unchanged whereas others had
321 been affected by the flame front. The overall results showed a decrease in volatile content and
322 subsequent changes in C, H, N, S and O depending on the sample, also fixed carbon and ash content
323 increased. SEM images confirmed the presence of char structures mixed with unchanged particles.
324 Char structures were larger than original particles as depicted by the comparison of size distribution of
325 original and residual samples. The implication of these results is that residues found after the
326 explosion were likely to be a proportion of dust pushed towards the vessel walls by the explosion
327 wind. As the flame front advanced particles were burnt in the flame front. But when the flame front
328 reached the wall and cooled down, particles closest to the wall remained largely unchanged whereas
329 those affected by the cooling flame were pyrolysed (as oxygen had been consumed in the flame front).
330 Residues therefore act as insulation and did not participate in the main combustion reaction;
331 consequently injected concentrations can be further corrected for a more accurate account of the
332 reacting dust concentration.

333 **Acknowledgements**

334 The authors are grateful to the Energy Program (Grant EP/H048839/1) for financial support. The
335 Energy Program is a Research Councils UK cross council initiative led by EPSRC and contributed to
336 by ESRC, NERC, BBSRC and STFC.

337 **References**

- 338 [1] World Coal Association, Coal and electricity generation, in: Coal Matters, World Coal
339 Association, London, 2012.
- 340 [2] DECC, Digest of UK energy statistics (DUKES), The Stationery Office, Norwich
- 341 [3] H. Nalbandian, Performance and risks of advanced pulverised coal plants, *Energieia*, 20 (2009).
- 342 [4] R.K. Eckhoff, *Dust Explosions in the Process Industries*, 3rd ed., Gulf Professional Publishing,
343 USA, 2003.
- 344 [5] K.N. Palmer, *Dust explosions and fire*, Chapman & Hall, London, 1973.
- 345 [6] J. Nagy, H.G. Dorsett, A.R. Cooper, Explosibility of carbonaceous dusts, in: R.I. 6597,
346 Washington, D.C., 1965, pp. p. 30.
- 347 [7] W. Cao, L. Huang, J. Zhang, S. Xu, S. Qiu, F. Pan, Research on Characteristic Parameters of
348 Coal-dust Explosion, *Procedia Engineering*, 45 (2012) 442-447.
- 349 [8] K.L. Cashdollar, Coal dust explosibility, *J. Loss. Prevent. Proc.*, 9 (1996) 65-76.
- 350 [9] B. Jensen, A. Gillies, Review of coal dust explosibility research, in: Australasian Institute of
351 Mining and Metallurgy, AusIMM, 1994, pp. 9-14.
- 352 [10] G. Continillo, S. Crescitelli, E. Furno, F. Napolitano, G. Russo, Coal dust explosions in a
353 spherical bomb, *J. Loss. Prevent. Proc.*, 4 (1991) 223-229.
- 354 [11] F. Woskoboenko, Explosibility of Victorian brown coal dust, *Fuel*, 67 (1988) 1062-1068.

- 355 [12] P.R. Amyotte, K.J. Mintz, M.J. Pegg, Y.-H. Sun, K.I. Wilkie, Laboratory investigation of the
356 dust explosibility characteristics of three Nova Scotia coals, *J. Loss. Prevent. Proc.*, 4 (1991) 102-109.
- 357 [13] C. Wilén, A. Moilanen, A. Rautalin, J. Torrent, E. Conde, R. Lödel, D. Carlson, P. Timmers, K.
358 Brehm, Safe handling of renewable fuels and fuel mixtures, in, VTT Technical Research Centre of
359 Finland, Espoo, 1999, pp. 117 p.+app. 118p.
- 360 [14] F. Norman, J. Berghmans, F. Verplaetsen, The Dust Explosion Characteristics of Coal Dust in an
361 Oxygen Enriched Atmosphere, *Procedia Engineering*, 45 (2012) 399-402.
- 362 [15] J.L. Krazinski, R.O. Buckius, H. Krier, Coal dust flames: A review and development of a model
363 for flame propagation, *Prog. Energy Combust. Sci.*, 5 (1979) 31-71.
- 364 [16] L.D. Smoot, D.T. Pratt, Pulverized coal combustion and gasification: Theory and applications for
365 continuous flow processes, Plenum Press, New York and London, 1979.
- 366 [17] A. Di Benedetto, P. Russo, Thermo-kinetic modelling of dust explosions, *J. Loss. Prevent. Proc.*,
367 20 (2007) 303-309.
- 368 [18] M. Hertzberg, I.A. Zlochower, K.L. Cashdollar, Volatility model for coal dust flame propagation
369 and extinguishment, *Symposium (International) on Combustion*, 21 (1988) 325-333.
- 370 [19] D. Bradley, G. Dixon-Lewis, S. El-Din Habik, Lean flammability limits and laminar burning
371 velocities of CH₄-air-graphite mixtures and fine coal dusts, *Combust. Flame*, 77 (1989) 41-50.
- 372 [20] International Organization of Standardization, Solid mineral fuels. Determination of gross
373 calorific value by the bomb calorimetric method and calculation of net calorific value, in, Geneva,
374 2009.
- 375 [21] R.J. Harris, The investigation and control of gas explosions and heating plant, E&FN Spon in
376 association with the British Gas Corporation, London, 1983.

377 [22] D.L. Ng, K.L. Cashdollar, M. Hertzberg, C.P. Lazzara, Electron Microscopy Studies of
378 Explosion and Fires Residues, in: IC 8936, Dept. of the Interior, Bureau of Mines, Washington D.C,
379 1983.

380 [23] K.L. Cashdollar, Overview of Dust Explosibility Characteristics, J. Loss. Prevent. Proc., 13
381 (2000) 183-199.

382 [24] V.I. Kuprianov, V. Tanetsakunvatana, Assessment of gaseous, PM and trace element emissions
383 from a 300-MW lignite-fired boiler unit for various fuel qualities, Fuel, 85 (2006) 2171-2179.

384 [25] P. Basu, Combustion and gasification in fluidised beds, CRC Press Taylor & Francis Group,
385 Boca Raton, FL, 2006.

386 [26] D.J.F. Slatter, C. Huescar Medina, H. Sattar, G. Andrews, H.N. Phylaktou, B.M. Gibbs, Biomass
387 explosion residue analysis, in: X International Symposium on Hazards, Prevention and Mitigation of
388 Industrial Explosions, Bergen, Norway, 2014.

389